

Dipole selection rules for optical transitions in the fcc and bcc lattices

W. Eberhardt

*Department of Physics, and Laboratory for Research on the Structure of Matter,
University of Pennsylvania, Philadelphia, Pennsylvania 19104*

F. J. Himpsel

Synchrotron Radiation Center, University of Wisconsin-Madison, Stoughton, Wisconsin 53589

(Received 10 September 1979)

We present the compilation of dipole selection rules for all high-symmetry points and lines of the fcc and bcc lattices, which can be used for the interpretation of absorption or photoemission data in the one-electron direct-transition picture.

Dipole selection rules have to be taken into consideration in the interpretation of optical-absorption and photoemission data. Structures in the optical-absorption data (e.g., in ϵ_2) are often interpreted in terms of a joint density of states, where transitions located at critical high-symmetry points give rise to

characteristic singularities. The same joint density of states model has been used to explain angle-integrated and also some angle-resolved photoemission data. The correct interpretation, however, at least in the one electron picture, involves a direct transition between electronic states of distinct sym-

TABLE I. High-symmetry points and lines of the cubic lattices.

Point	Coordinates			Symmetry group	Table No.
A. Inside the Brillouin zone					
Γ	0	0	0	O_h	II
Δ	k_x	0	0	C_{4v}	III
Σ	$k_x = k_y$		0	C_{2v}	IV
Λ	$k_x = k_y = k_z$			C_{3v}	V
B. Surface of bcc Brillouin zone					
H	$2\pi/a$	0	0	O_h	II
N	π/a	π/a	0	D_{2h}	VI
P	π/a	π/a	π/a	T_d	VIII
D	π/a	π/a	k_z	C_{2v}	IV
G	$(2\pi/a - k_y)$	k_y	0	C_{2v}	IV
F	$(2\pi/a - k_y)$	$k_y = k_z$		C_{3v}	V
C. Surface of fcc Brillouin zone					
X	$2\pi/a$	0	0	D_{4h}	VII
K	$3\pi/2a$	$3\pi/2a$	0	C_{2v}	IV
L	π/a	π/a	π/a	D_{3d}	IX
U	$2\pi/a$	$\pi/2a$	$\pi/2a$	C_{2v}	IV
S	$2\pi/a$	$k_y = k_z$		C_{2v}	IV
Z	$2\pi/a$	k_y	0	C_{2v}	IV
W	$2\pi/a$	π/a	0	D_{2d}	X

TABLE II. Allowed dipole transitions (+) at Γ and H . $\vec{A} \cdot \vec{p}$ is represented by Γ_{15} .

O_h	Γ_1	Γ_2	Γ_{12}	$\Gamma_{15'}$	$\Gamma_{25'}$	$\Gamma_{1'}$	$\Gamma_{2'}$	$\Gamma_{12'}$	Γ_{15}	Γ_{25}
Γ_1	+	...
Γ_2	+
Γ_{12}	+	+
$\Gamma_{15'}$	+	...	+	+	+
$\Gamma_{25'}$	+	+	+	+
$\Gamma_{1'}$	+
$\Gamma_{2'}$	+
$\Gamma_{12'}$	+	+
Γ_{15}	+	...	+	+	+
Γ_{25}	...	+	+	+	+

metries. Therefore, dipole selection rules are important and have to be taken into consideration, especially when polarized radiation is used for the optical excitation. Recently it has been shown that in angle-resolved photoemission, one is able to localize the transitions at high-symmetry points of the band structure. In these data, the importance of the dipole selection rules can be seen directly.

An application of the dipole selection rules in the specialized form of photoemission in a mirror plane^{1,2} or in the direction of the surface normal³⁻⁶ can be found in the literature. Polarization effects in core-level excitations have been discussed for GaAs(110), where the importance of the dipole selection rules is shown in an indirect but very nice way.⁷ Recently, those selection rules have been applied and verified throughout the Brillouin zone in the case of Ni,

where all high-symmetry points of the bands have been determined using angle-resolved photoemission in connection with the polarization of the synchrotron radiation.⁸ The effect of the dipole selection rules is also reflected in the direct calculation of the optical transition matrix elements for Cu.⁹

The dipole selection rules are not restricted in application to bulk bands, but also can be verified for ordered adsorbate overlayers. This has been treated theoretically¹⁰ and has been applied especially for CO on Ni(100),^{11,12} and O on Al(111),¹³ to give two clear cut examples.

The transition matrix element relevant for absorption as well as photoemission data can be written in the form $\langle f | \vec{A} \cdot \vec{p} + \vec{p} \cdot \vec{A} | i \rangle$. If we neglect local field effects,¹⁴ this reduces to $\langle f | \vec{A} \cdot \vec{p} | i \rangle$ where $\langle f |$ and $| i \rangle$ are the final and initial state of the electron and $\vec{A} \cdot \vec{p}$ is the dipole operator. In order to find out

TABLE III. Allowed dipole transitions at Δ . (+) is for \vec{A} parallel Δ ; $\vec{A} \cdot \vec{p}$ is represented by Δ_1 . (0) is for \vec{A} normal Δ ; $\vec{A} \cdot \vec{p}$ is represented by Δ_5 .

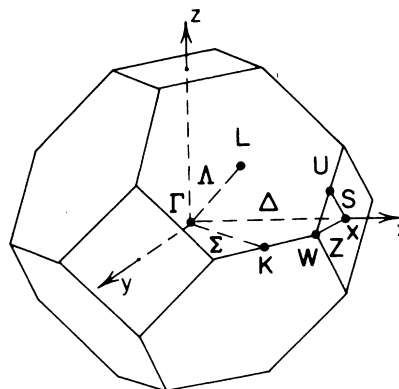
C_{4v}	Δ_1	$\Delta_{1'}$	Δ_2	$\Delta_{2'}$	Δ_5
Δ_1	+	0
$\Delta_{1'}$...	+	0
Δ_2	+	...	0
$\Delta_{2'}$	+	0
Δ_5	0	0	0	0	+

TABLE IV. Allowed dipole transitions at Σ , D , G , K , U , S , and Z . (+) is for \vec{A} parallel Σ ; $\vec{A} \cdot \vec{p}$ is represented by Σ_1 . (0) is for \vec{A} normal Σ , parallel x ; $\vec{A} \cdot \vec{p}$ is represented by Σ_3 . (X) is for \vec{A} normal Σ , parallel y ; $\vec{A} \cdot \vec{p}$ is represented by Σ_4 .

C_{2v}	Σ_1	Σ_2	Σ_3	Σ_4
Σ_1	+	...	0	X
Σ_2	...	+	X	0
Σ_3	0	X	+	...
Σ_4	X	0	...	+

TABLE V. Allowed dipole transitions at Λ and F . (+) is for \vec{A} parallel Λ ; $\vec{A} \cdot \vec{p}$ is represented by Λ_1 . (0) is for \vec{A} normal Λ ; $\vec{A} \cdot \vec{p}$ is represented by Λ_3 .

C_{3v}	Λ_1	Λ_2	Λ_3
Λ_1	+	...	0
Λ_2	...	+	0
Λ_3	0	0	+0



whether this matrix element describes a dipole allowed transition, we can apply the rules of group theory. If we consider a transition located at a high-symmetry point or line of the Brillouin zone, then all the wave functions, the dipole operator, and the whole transition matrix element transform like the representations of the corresponding group. The matrix element in general is invariant under all symmetry operations. This implies that a nonvanishing matrix element contains the unity representation. Therefore, for an allowed transition, the direct product of the representations of the initial state, and final state, and the dipole operator contains the unity representation.

This is equivalent to the statement that the direct product of the representations of the initial and final state wave functions contains the representation of the dipole operator. This can be checked by looking

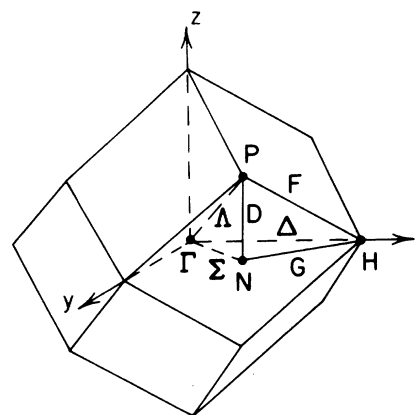


FIG. 1. Brillouin zones of the body-centered-cubic (bcc) and face-centered-cubic (fcc) lattices. The high-symmetry points and lines are indicated.

TABLE VI. Allowed dipole transitions at N . (+) is for \vec{A} parallel X ; $\vec{A} \cdot \vec{p}$ is represented by $N_{2'}$. (X) is for \vec{A} parallel Y ; $\vec{A} \cdot \vec{p}$ is represented by $N_{3'}$. (0) is for \vec{A} parallel Z ; $\vec{A} \cdot \vec{p}$ is represented by $N_{4'}$.

D_{2h}	N_1	N_2	N_3	N_4	$N_{1'}$	$N_{2'}$	$N_{3'}$	$N_{4'}$
N_1	+	X	0
N_2	+	...	0	X
N_3	X	0	...	+
N_4	0	X	+	...
$N_{1'}$...	+	X	0
$N_{2'}$	+	...	0	X
$N_{3'}$	X	0	...	+
$N_{4'}$	0	X	+

TABLE VII. Allowed dipole transitions at X . (+) is for \bar{A} parallel Δ ; $\bar{A} \cdot \bar{p}$ is represented by $X_{4'}$. (0) is for \bar{A} normal Δ ; $\bar{A} \cdot \bar{p}$ is represented by $X_{5'}$.

D_{4h}	X_1	X_2	X_3	X_4	$X_{1'}$	$X_{2'}$	$X_{3'}$	$X_{4'}$	X_5	$X_{5'}$
X_1	+	...	0
X_2	+	0
X_3	+	0
X_4	+	0
$X_{1'}$	+	0	...
$X_{2'}$	+	0	...
$X_{3'}$...	+	0	...
$X_{4'}$	+	0	...
X_5	0	0	0	0	...	+
$X_{5'}$	0	0	0	0	+	...

TABLE VIII. Allowed dipole transitions (+) at P ; $\bar{A} \cdot \bar{p}$ is represented by P_4 .

T_d	P_1	P_2	P_3	P_4	P_5
P_1	+	...
P_2	+
P_3	+	+
P_4	+	...	+	+	+
P_5	...	+	+	+	+

TABLE IX. Allowed dipole transitions at L . (+) is for \bar{A} parallel Λ ; $\bar{A} \cdot \bar{p}$ is represented by $L_{2'}$. (0) is for \bar{A} normal Λ ; $\bar{A} \cdot \bar{p}$ is represented by $L_{3'}$.

D_{3d}	L_1	L_2	L_3	$L_{1'}$	$L_{2'}$	$L_{3'}$
L_1	+	0
L_2	+	...	0
L_3	0	0	0+
$L_{1'}$...	+	0
$L_{2'}$	+	...	0
$L_{3'}$	0	0	0+

at the characters of the representations involved. The characters form a linear independent set of basis vectors for the vector space of the dimension of the group. Therefore, it can be easily checked, whether the product of the representation of the initial state and the final states contains or is equal to the representation of the dipole operator.

We have determined all possible dipole transitions at the high-symmetry points and lines of the face-centered-cubic (fcc) and body-centered-cubic (bcc) lattices. The two corresponding Brillouin zones are shown in Fig. 1. In Table I, we give the high-symmetry points and lines, their locations, and the

TABLE X. Allowed dipole transitions at W . (+) is for \bar{A} parallel Z ; $\bar{A} \cdot \bar{p}$ is represented by $W_{2'}$. (0) is for \bar{A} normal Z ; $\bar{A} \cdot \bar{p}$ is represented by W_3 .

D_{2d}	W_1	$W_{1'}$	W_2	$W_{2'}$	W_3
W_1	+	0
$W_{1'}$	+	...	0
W_2	...	+	0
$W_{2'}$	+	0
W_3	0	0	0	0	+

corresponding symmetry groups. The allowed dipole transitions for various directions of the polarization vector of the electric field are tabulated in Tables II–X. These tables deal with the dipole transition only. For a comparison with angle-resolved photoemission data, one has to take into account what final states can contribute to the photoemission process. In normal photoemission along Δ , Σ , or Λ it is known that the final state has to be totally symmetric (Δ_1 , Σ_1 , or Λ_1). Under these conditions our tables reduce to the one given by Hermanson earlier.³ Similar tables can be obtained for the hcp lattice. A compilation for selection rules of an hcp lattice is published elsewhere.¹⁵

For the general case of an angle-resolving detector in off-normal photoemission the final states contribute according to a golden rule-type matrix ele-

ment.^{16,17} This matrix element contains a time-reversed LEED (low-energy electron diffraction) final state, which is characterized by the reduced momentum parallel to the surface, \bar{k}_{\parallel} . Bloch states which contribute to this time-reversed LEED state have the same reduced \bar{k}_{\parallel} and are invariant with respect to all symmetry operations leaving the position of the detector unaffected. For the case of emission in a mirror plane it follows that contributing final Bloch states have to be even with respect to that mirror plane. At the boundary of the surface Brillouin zone, surface lattice vectors play a role in determining the symmetry of possible final Bloch states.⁴

This work was supported by the NSF through the Materials Research Laboratory program under Grant No. DMR-76-80944 and NSF Grant No. DMR-73-02656.

¹E. Dietz, H. Becker, and U. Gerhardt, Phys. Rev. B **12**, 2084 (1975); Phys. Rev. Lett. **36**, 1397 (1976).

²E. W. Plummer and W. Eberhardt, Phys. Rev. B **20**, 1444 (1979).

³J. Hermanson, Solid State Commun. **22**, 9 (1977).

⁴F. J. Himpfel and W. Steinmann, Phys. Rev. B **17**, 2537 (1978).

⁵F. J. Himpfel, J. A. Knapp, and D. E. Eastman, Phys. Rev. B **19**, 2919 (1979).

⁶P. Thiry, D. Chandresris, J. Lecante, C. Guillot, R. Pinchaux, and Y. Pétroff, Phys. Rev. Lett. **43**, 82 (1979).

⁷G. J. Lapeyre and J. Anderson, Phys. Rev. Lett. **35**, 117 (1975).

⁸W. Eberhardt and E. W. Plummer, Phys. Rev. B **21**, 3245 (1980).

⁹N. V. Smith, Phys. Rev. B **19**, 5019 (1979).

¹⁰M. Scheffler, K. Kambe, and F. Forstmann, Solid State Commun. **25**, 93 (1978).

¹¹R. J. Smith, J. Anderson, and G. J. Lapeyre, Phys. Rev. Lett. **37**, 1081 (1976).

¹²C. Allyn, T. Gustafsson, and E. W. Plummer (unpublished).

¹³W. Eberhardt and F. J. Himpfel, Phys. Rev. Lett. **42**, 1375 (1979).

¹⁴K. L. Kliewer, Phys. Rev. B **14**, 1412 (1976).

¹⁵F. J. Himpfel and D. E. Eastman, Phys. Rev. B **21**, 3207 (1980); and J. F. Cornwell, Phys. Kondens. Mater. **4**, 327 (1966).

¹⁶I. Adawi, Phys. Rev. **134**, A788 (1964).

¹⁷G. D. Mahan, Phys. Rev. B **2**, 4334 (1970).